



Published in final edited form as:

Ind Eng Chem Res. 2010 May 19; 49: 4687–4693. doi:10.1021/ie901580k.

Sulfur-Functionalization of Porous Silica Particles and Application to Mercury Vapor Sorption

Noah D. Meeks, Stephen Rankin, Dibakar Bhattacharyya*

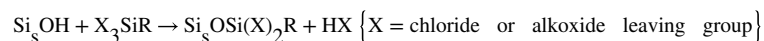
University of Kentucky, Department of Chemical and Materials Engineering, Lexington, Kentucky 40506

Abstract

Silanol (SiOH) groups on silica particle surfaces undergo silylation reactions with organosilane molecules to give functionalized particles, which are used in many applications. The determination of the extent of this reaction is important for proper design of functionalized materials, depending upon the application. Two types of porous silica particles (206 and 484 m² g⁻¹; 9.6 and 2.9 nm average pore diameter, respectively), and colloidal silica (Ludox) with a nonporous base particle of 22 nm diameter, were functionalized with sulfur-containing silanes, 3-mercaptopropyl trimethoxy silane (MPTMS), and bis[3-(triethoxysilyl) propyl]-tetrasulfide (S4). Maximum extent of functionalization was determined with S4 using Fourier transform infrared spectrometry (FTIR), thermogravimetric analysis (TGA), and total S analysis. For the two types of porous silica particles, FTIR indicated that 54 and 17% of the silanol groups were functionalized with S4, and TGA indicated that the functionalized particles were 12 and 11 mass % MPTMS, respectively. These results were independently confirmed with total sulfur analysis. Extents of functionalization were determined for varying the silane structure on the same silica particle. MPTMS reacted with 38% of functional groups, while S4 reacted with 17%; the mass % of silane is the same regardless of silane structure on the same silica particle. Characterization by DSC indicated a glass transition occurs in the silane layer of the S4-functionalized silica at about 85 °C, but not in the MPTMS functionalized particles. Finally, mercury sorption breakthrough curves indicate the pore characteristics of the S4 functionalized samples.

1. Introduction

Surface functionalization of porous silica particles with organosilanes (silylation) is an important area in many fields of the chemical industry. The heart of silica surface functionalization involves the formation of covalent bonds between silica surface hydroxyl groups (silanol groups) and the Si center of a chloro- or alkoxysilane molecule:



The resulting surface Si–O–Si–C linkages provide good thermal and chemical stability¹ (including stability due to the coatings which increase hydrophobicity^{2,3}). These silylation

*To whom correspondence should be addressed. db@engr.uky.edu. Tel.: 859-257-2794. Fax: 859-323-1929. Address: Dept. of Chemical and Materials Engineering, University of Kentucky, 177 Anderson Hall, Lexington, KY 40506-0046.

reactions have been used to form functionalized silica particles for chromatograph columns, ^{4,5} catalysts, ^{6,7} and other products. Two different routes to achieve the functionalized particles are available. Silylation can be done at the monomer level, and then the functional monomers are co-condensed with silica precursors to form functional particles, ^{8,9} or the silanol groups of already-formed silica particles can be functionalized. The latter strategy (sometimes called grafting) is used in this study. Two silylation mechanisms have been proposed. ^{10,11} The first is the widely accepted sol–gel mechanism, in which moisture (either added or adsorbed to silica particles stored under atmospheric conditions) hydrolyzes the chloro- or alkoxy-leaving groups of the silane, followed by condensation with surface silanol groups. ^{12,13} One recent study ¹⁴ has shown that it is even possible to exploit this mechanism in a solventless silylation process. The second mechanism that has been proposed is a direct one-step nucleophilic substitution mechanism believed to sometimes operate during vapor phase silylation in a dry atmosphere. ¹⁵

The use of functionalized silica particles has been proposed for separations with environmental applications, such as removal of mercury ^{16–19} from contaminated aqueous streams using thiol-functionalized silica particles, copper removal using amine-functionalized silica particles, ²⁰ and removal of pentachlorophenol (PCP) from water using surface-imprinted amine-functionalized silica particles. ²¹ Environmental applications of functionalized silica particles are not limited to aqueous systems. Sulfonic acid groups on functionalized silica particles were used to remove dibenzothiophene (DBT) from octane after exchanging H⁺ for Ag⁺. ²² In vapor phase environmental applications, our lab recently proposed ²³ using a sulfur/siloxane network (formed from a tetrasulfur-bridged silane) for the capture of elemental vapor phase mercury at elevated temperature. This was proposed because MPTMS-functionalized silica (as used for Hg²⁺ sorption) had been previously shown as ineffective for elemental Hg vapor sorption. ²⁴ Another proposed application of functionalized silica particles is the generation of methyl chloride for calibration of instruments dealing with environmental monitoring. ²⁵

Recently there has been much interest in effective noncarbon mercury vapor sorbents, ^{26,27} as well as interest of mercury sorption technology in general. ²⁸ Activated carbons are conventionally used for this application, but they have the disadvantages: the physisorption mechanism decreases capacity at higher temperatures, and the SO₃ present in flue gas streams interferes with the sorption on activated carbon. These conventional sorbents have also been shown as ineffective toward Hg sorption in flue gases from low-Cl coals, and halogenated powdered activated carbon (PAC) has been used to bind elemental mercury by surface-enhanced oxidation using other adsorbed species followed by chelation with the halogen. ²⁹ Silica–titania nanocomposites have been shown to have increased capacity (average of 10 mg Hg g⁻¹ sorbent) over activated carbon. ²⁷ Also, a thiol-functionalized silica coated with an immobilized ionizing liquid is reported to have a capacity of 12 mg Hg g⁻¹ sorbent, ³⁰ but this material must be used at lower temperatures (135 °C maximum). A recent study in our lab ³¹ has demonstrated the use of copper in conjunction with a tetrasulfur moiety (but on a nonsilica support) to promote the capture of elemental vapor phase Hg, and it has been hypothesized that the copper acts to arrange or align the sulfur atoms in a geometry which is more conducive to Hg capture. This alignment may result in a sulfur network with improved mass transfer of Hg to the network interior compared to oxide

particles without copper. Further, the effective use of sulfur function-lization on copper-doped silica particles for adsorption of elemental vapor phase Hg has recently been demonstrated in our lab, with capacities of over 20 mg Hg g⁻¹ sorbent.³²

The objective of this paper is to understand the extent of sulfur functionalization of silica particles based upon silica particle and silane structural parameters. A second objective of this paper is to characterize sulfur-functionalized silica particles demonstrating thermal stability. Third, brief mercury vapor sorption results of the sulfur-functionalized particles are presented and related to the structural parameters of the silica particles. Our previous publications^{23,24,31,32} have dealt primarily with mercury capture studies rather than understanding the silylation reaction involving tetrasulfur silane.

2. Materials and Methods

2.1. Materials Used.

Silica particles having various structure parameters given in Table 1 were obtained from J. M. Huber Corporation (Havre de Grace, MD) for silicas A and B; Ludox colloidal silica (TM-50) was obtained from Grace Davison (Columbia, MD). Sulfur-containing silane reagents used were 95% 3-mercaptopropyltrimethoxysilane (MPTMS) or 95% bis[3-(triethoxysilyl) propyl]tetrasulfide (S4) (Figure 1), which were obtained from Sigma-Aldrich, Inc. (St. Louis, MO) and Gelest, Inc. (Morristown, PA), respectively.

2.2. Silylation Procedure.

Silica particles were functionalized by adding 2.5 g of particles and 0.9 mL of silane into a flask containing enough anhydrous ethanol to disperse the particles (ca. 50 mL). The mixture was heated to 80 °C to evaporate the ethanol, and the remaining moist silica was heated at 110 °C for at least 4 h in order to accomplish silylation. The particles were then washed with ethanol under vacuum filtration using a 0.45 μm filter membrane and dried at 80 °C overnight.

2.3. Determination of Extent of Functionalization.

Three methods are used to determine the extent of functionalization of the various silica particles using sulfur-containing silanes. First, Fourier transform infrared spectrometry (FTIR) was used: a small amount (ca. 5–10 mg) of the functionalized silica was ground with KBr and pressed into a pellet. A KBr pellet containing a similar amount of unfunctionalized silica was also prepared, and the spectra of both were acquired using a Thermo-Nicolet Nexus 470 spectrometer running Omnic software.

The second method of determining the extent of silylation is to use thermogravimetric analysis (TGA) to determine the weight percent of the functionalized particles which is silane. The TGA plots of the unfunctionalized particles are compared to those of the functionalized particles in order to properly account for the weight loss due to moisture evaporation in all the silica samples. The TGA experiments were carried out by loading ca. 20 mg sample into the TA Instruments Hi Res TGA 2950 equipped with an EGA furnace and heating to 1000 °C at a rate of 10 °C min⁻¹ in a Pt pan under an air flow rate of 120 mL

min⁻¹. The third method for determining the extent of functionalization is total sulfur analysis, which also operates by heating the sample. Instead of measuring the mass loss as in TGA, a small sample was heated in an Eltra total sulfur analyzer which determines the mass percent of sulfur based on infrared analysis of the combustion products (sulfur oxides).

2.4. Characterization of Functionalized Particles.

Nitrogen sorption isotherms were collected at 77 K for all functionalized and unfunctionalized samples using a Micromeritics Tristar 3000, and pore volume distributions were calculated by Tristar 3000 V 4.02 software using the BJH method.

Differential scanning calorimetry (DSC) analyses were conducted on MPTMS- and S4-functionalized silica A particles to demonstrate that there is a cross-linked network on the S4-functionalized particles but not on the thiol-functionalized particles. Approximately 5–10 mg of particles were heated to 130 °C then cooled to 30 °C in order to remove excess moisture. The same samples were reheated to 300 °C at a rate of 5 °C min⁻¹ in a Pt-Rh alloy pan under an N₂ atmosphere, and the heat flow was measured. The baseline DSC plot for an empty pan was subtracted.

2.5. Determination of Mercury Capture Efficiency.

Mercury capture efficacy was determined using a packed bed experiment, which has been described in detail elsewhere.³² A Vici-metrics mercury emitter cell (1454 ng Hg min⁻¹ at 100 °C) was used as a mercury source, and it was diluted into a stream of nitrogen flowing 60 mL min⁻¹. The dilute mercury gas flowed through the packed bed which was held at 140 °C by immersion in a silicone oil bath. The outlet concentration of mercury was determined using a model 400 cold vapor mercury analyzer from Buck Scientific. To confirm the results of the online-mercury analyzer, the packed bed was digested in 25 mL of a 4:1 mixture of 16 M nitric acid and 8 M hydrochloric acid. After overnight digestion, the mixture was diluted with deionized ultrafiltered (DIUF) water. The remaining solid particles were removed by syringe filtering through a 0.45 μm PVDF membrane. The concentration of mercury in the supernatant was determined by preparing standard solutions and analyzing using a Varian Vista Pro ICP–OES. The lowest detectable concentration for Hg²⁺ ion for this method is 0.5 ppm.

3. Results and Discussion

The first objective of this study is to determine the effect that silica particle structure and silane structure have with regard to the maximum extent of silica particle functionalization, using IR, Ag⁺ sorption, TGA, and thermal swing adsorption (TSA). The second objective is the thermal characterization of the functionalized silica particles. The third objective is to demonstrate how pore structures influence breakthrough capacity of these sulfur-functionalized particles.

3.1. Effect of Silica Particle Structure on Extent of Functionalization.

The three types of silica particles used in this study (Table 1) were chosen because of their different structural characteristics. The surface areas and average pore diameters of the S4-

functionalized silicas are also given in Table 1. Silica A and silica B are both porous silica gels with similar particle diameters; Ludox (TM-50) is colloidal silica with monodisperse primary particles 22 nm in diameter (provided by manufacturer but confirmed by our lab using dynamic light scattering and SEM). Nitrogen sorption isotherms (Figure 2a,c) for these samples are IUPAC Type IV, confirming the porous nature of the sample.³³ Silica A has a much larger hysteresis than silica B due to the larger mesopores. Although the Ludox base particles (22 nm) are nonporous, the small diameter allows for close packed aggregates of particles, which leads to small “pores” between particles. The nitrogen sorption isotherms and pore distributions for the functionalized particles (Figure 2b,d) are described below. The extent of S4 functionalization on these different particles is compared using infrared spectroscopy and/or thermogravimetric analysis.

A representative FTIR spectrum of S4-functionalized silica is shown in Figure 3. The IR peak at 980 cm^{-1} , which is attributed to the Si–O–H vibration, can be used to determine the extent of functionalization.³⁴ The FTIR spectra are normalized using the Si–O–Si peak (normalized to the bulk amount of silica), then the difference in peak height between the functionalized and unfunctionalized silica at 980 cm^{-1} is proportional to the extent of functionalization. Since the amount of silica (based upon Si–O–Si peak height) has been normalized for both samples, small differences in the mass of sample used to prepare the pellets can be neglected, and any difference in Si–O–H peak height between the functionalized and unfunctionalized samples is attributed to the disappearance of silanol groups during the silylation reaction. Although the silylation reaction does result in the formation of new siloxane bonds, the number of bonds formed relative to the total amount in the bulk sample is expected to be 2 orders of magnitude lower, even with the high surface area of the silica.

The extent of functionalization results are summarized in Table 2. Silica B has a much larger specific surface area; it may be expected that the larger surface area should allow for a greater extent of silylation. However, silica A has 54% of its silanols functionalized with S4, with a standard deviation of 8.8% of the silanols functionalized (for three different silylation batches). For silica B, the extent of silylation with S4 is 17% with a standard deviation of 4.2% of the silanols functionalized. These results indicate that the larger pores of silica A allow for the silane to reach a higher percentage of the reactive silanol sites. For the Ludox samples, the IR spectral noise was too great to quantify the extent of silylation, but TGA and total S were used for these materials.

While IR measures extent of functionalization in terms of how many silanol are reacted, TGA measures extent of functionalization in terms of how much silane can be deposited onto the surface and into the pores of silicas A and B. A representative TGA plot is shown in Figure 4. TGA results indicate that silica A has a greater mass of silane deposited on it (12.0 wt % silane with standard deviation of 1.6 wt %) than silica B (11.0 wt % silane with standard deviation of 0.4%). These values are of the same magnitude as previously reported values using the same method.³⁵ In the small pores of silica B, both ends are more likely to react with the surface, which would lead to a loss of more SiOH per S4 molecule incorporated. Although silica B has fewer % silanol groups reacted, the high surface area allows it to react with a large mass of silane, and there is some multilayer deposition as well.

When the mass % silane for silicas A and B is normalized by the factor of surface area \times % silanol reacted, the ratio of normalized S4-silica A to normalized S4-silica B is 1.24. So at least 20% more silane is present on the S4-silica B than would be expected based on its surface area and the amount present on S4-silica A. The S4-functionalized Ludox has an average of 4.7 wt % silane (standard deviation of 0.2 wt %) because the Ludox surface area (where the silane can attach) is much smaller. Similar to the TGA method, total sulfur analysis gives the extent of functionalization in terms of total sulfur mass whether those sulfur-containing silanes are covalently bound to the surface or deposited into the pores. Silica A has 4.53 mass % sulfur, and silica B has 3.98 mass % sulfur. Consistent with the TGA results, Ludox has 1.56 mass % sulfur. The total S analysis gives a systematically higher value for S than would be expected based on the TGA (by converting mass % silane to mass % S) for two reasons. First, the S is higher than would be expected because the mass of silane remaining on the particle is less than the mass of the original silane (due to alkoxy leaving group). Second, the commercial silica gels silica A and B have a small amount of sodium sulfate as an artifact of their manufacture.

Pore volume distributions have been calculated with the BJH method (Figure 2b,d). For silica A, silylation occurs more easily in the larger mesopores with silane, and the average pore diameter is reduced from 9.6 nm to less than 3.3 nm, as the pore walls are coated with the silane. However, these narrower pores still have larger surface area, and the addition of S4 actually increases the surface area to $264 \text{ m}^2 \text{ g}^{-1}$, suggesting that the S4 is able to form a network on the surface with very small pores. This explanation is also consistent with the order of magnitude decrease in average pore diameter. The silylation of Ludox (4.7 wt % silane) fills in the gaps between particles and results in an agglomeration of particles and the silane network, and the apparent “pore” volume is also reduced for Ludox particles with silylation. However, this agglomeration also produces a porous silane network which contains the particles, as the surface area is increased to $243 \text{ m}^2 \text{ g}^{-1}$. Silylation of silica B leads to a decrease in mesopores of all sizes, and the large decrease in surface area (484 to $61 \text{ m}^2 \text{ g}^{-1}$) arises from the complete blocking of the silica particles’ pores by the large S4. The occurrence of pores after S4 functionalization is greatly decreased. However, most of the remaining porosity arises from the porous S4 network. For all the functionalized materials, the porosity and surface area occur from two sources, one from the silica itself and one from the S4 deposited on the surface. In the case of silica A and Ludox, the functionalization reaction enhanced the surface area. In the case of silica B, the silylation first covered the smaller pore openings, dramatically reducing the surface area. The silanized particles were covered in additional silane network (S4), which although having very few pores, increased the nominal pore diameter.

3.2. Impact of Silane Molecule Structure on Extent of Functionalization.

A second objective of this study is to determine the difference in extent of silica particle functionalization achieved with different silanes. The two silanes which are considered are S4 (with results discussed in the previous section) and MPTMS (Figure 1). These silanes react with the particle surface through a single silicon center (“single-point attachment”) in the case of MPTMS or through one or two silicon centers (“double point attachment”) in the case of S4. Silica B is the silica that is functionalized in this comparison. Based on the extent

of silylation determined using IR spectroscopy, MPTMS reacted with an average of 38% of silanol groups, with a standard deviation of 8.6 for the three different samples which were prepared. However, using the same method, S4 reacted with an average of 17% of silanol groups, with a standard deviation of 4.2, also for 3 different samples. This difference based on the structure of the silanes is expected because the MPTMS functionalizes the silica by one end only. However, the S4 can react with the particle surface at two different locations and hinders further reaction with other silanol groups and block pore openings.

TGA results indicate that silane reacted with the silica particle surface is approximately the same for both MPTMS (10.6 mass %) and S4 (11.0 mass%) silanes, as the silica particle characteristics are the same in both cases. Total sulfur analysis also confirms this result. The extent of functionalization is not dependent on the structure of the silane molecule for this silica particle with small pores. On the basis of these results taken together (and converting the mass to moles from the TGA results), it is concluded that not all of the S4 react at both ends. The mole % of S4 on silica A is 1.7. Considering that for double-point attachment, 2 SiOH are consumed for every S4 added, 3.4 mols SiOH should be reacted in the S4 case. For the MPTMS case, the mole % of MPTMS on silica A is 4.9 (and also 4.9 mols SiOH consumed). Thus, for MPTMS, 4.9 mols SiOH react, and 3.4 mols of SiOH should react with S4. However, the IR results would indicate that approximately twice as many silanol groups are reacted with MPTMS as with S4, indicating a portion of the S4 does not have double-point attachment.

3.3. DSC Characterization.

The functionalized particles were analyzed using differential scanning calorimetry in order to determine if the sulfur-containing silanes exhibited any thermal transitions. This is of interest because the mercury sorption scheme is proposed to operate at about 140 °C. Although both the heating and cooling scans were obtained for completeness, the cooling scan is more typically used for glass transition identification³⁶ and is shown in Figure 5. For the S4-functionalized silica particles, a slight glass transition is observed at 85 °C, and the step in the plot is validated by the derivative DSC plot. This transition is not as strongly observed for the MPTMS-functionalized silica particles. It is proposed that the S4 chains can interact with each other on the surface and act as a polymer network, whereas the reduced thiol groups do not interact on the silica particle surface, although some oxidation of the -SH to S-S could occur. Also, it is possible that some of the S4 molecules (with two reactive ends) formed oligomers prior to reaction with the silica particle surface. Further understanding of this network will be important to elucidating the mechanism for mercury capture using these materials.

3.4. Application to Mercury Vapor Sorption.

Lab-scale mercury capture experiments were conducted to relate the Hg sorption to the pore structure before and after functionalization. The use of sulfur (in various forms) as a sorbent for mercury is well-known, although the structure of the active site of sorption for this tetrasulfane and mercury is unclear. In this study, the S4-functionalized materials were used for mercury sorption. The total capacity for S4-functionalized silica A was 160 $\mu\text{g Hg g}^{-1}$ silica, but the other S4-functionalized sorbents had very low Hg sorption capacities (less

than $10 \mu\text{g Hg g}^{-1}$ silica). The highly accessible surface area of the S4-silica A allows for the higher capacity. S4-Ludox also has a high surface area but that is primarily due to the S4 network around the particles, which indicates that S4 is more dispersed and perhaps the oligomers are better aligned on the silica with high surface area and large pore diameters. In this study, the primary objective was not directed toward achieving high mercury capacity but material synthesis and characterization. High capacities have been shown by our previous publication using S4-functionalized silica to which small amounts of copper sulfate have been added. It is expected that the copper sulfate allows for even a much better dispersion of the S4.³²

For sorption, the breakthrough curves give information about the accessibility of active sites to the sorbate. Figure 6 shows the four breakthrough curves (shown only for $C/C_0 > 0$). The steeper the breakthrough is, the more accessible and open-structured are the sites. The steeper breakthrough curves indicate less mass transfer resistance, which is desirable for applications involving short residence times. S4-Ludox has the steepest breakthrough, but S4-silica A has the most gradual breakthrough, even though both these materials have almost identical pore distributions and surface areas. However, the difference in these two materials is that much more of the surface area in S4-Ludox arises directly from the S4 network, so the active sites are much more accessible. S4-Silica A also has a very gradual breakthrough at high C/C_0 indicating the high resistance to filling the microporous active sites. Similarly, S4-silica B has a breakthrough curve which follows closely along the S4-Ludox curve (facile mass transfer due to the S4 covering the pore mouths), but near maximum capacity ($C/C_0 > 0.9$) the curve becomes much more gradual as the few remaining microporous sites slowly become occupied. The breakthrough curves shown do not indicate the capacity of the material, only the openness of the functionalized material's pore structure. Only S4-silica A showed significant capacity. Most of the capacity is determined by the time before breakthrough.

4. Conclusions

This study has focused on determining the extent of silylation that can be achieved on the surface of porous amorphous silica particles with various characteristics. Unlike many previous studies which focus on ideal particles, this work has determined extents of reaction for commercially available silica particles which are currently used in various industries, for applications besides mercury sorption. Different methods have been used to determine the extent of functionalization, and it has been shown that up to 50% of the silica surface silanol groups can be functionalized, even with a bridged silane that can attach to the particle surface through two silicon centers. The extent of silylation reaction has been shown to be primarily dependent upon pore distribution, size of the silane, and whether the silane is monofunctional or difunctional. The extent of functionalization (as deposition) depends on pore volume and is also not affected by the structure of the silane. These particles have good thermal stability in the temperature range of interest, and the formation of sulfur-containing oligomers on the silica particle surface has been indicated. The future prospects for work in this area are promising, especially the elucidation of the mercury adsorption mechanism on the surface of the functionalized particles and the structure of the S4 silane on the particle surface.

Acknowledgment

This work was funded by J. M. Huber Corporation (Havre de Grace, MD). Part of the silica functionalization work was also supported by the NIEHS-SRP (P42ES007380) program. The authors acknowledge the analytical assistance of Tricia Coakley at UK Environmental Research and Training Laboratories (ERTL), and Prof. John Selegue at UK Department of Chemistry. The mercury detector was provided by the U.S. Environmental Protection Agency.

Literature Cited

- (1). Iler RK *The Chemistry of Silica*; Wiley: New York, 1979.
- (2). Etienne M; Walcarius A Analytical investigation of the chemical reactivity and stability of aminopropyl-grafted silica in aqueous medium. *Talanta* 2003, 59, 1173–1188. [PubMed: 18969008]
- (3). Park DH; Nishiyama N; Egashira Y; Ueyama K Enhancement of hydrothermal stability and hydrophobicity of a silica MCM-48 membrane by silylation. *Ind. Eng. Chem. Res* 2001, 40, 6105–6110.
- (4). Ma YR; Qi LM; Ma JM; Wu YQ; Liu O; Cheng HM Large-pore mesoporous silica spheres: Synthesis and application in HPLC. *Colloids Surf., A* 2003, 229, 1–8.
- (5). Galli B; Gasparrini F; Misiti D; Natile G; Palmieri G Thin-layer chromatography of metal-complexes on glycidoxypopyl functionalized silica plates. *J. Chromatogr* 1987, 409, 377–382.
- (6). Revillon A; Leroux D Functional silica supported polymer. 5. ‘Onto’ versus ‘from’ grafting processes. *React. Funct. Polym* 1995, 26, 105–118.
- (7). Iiskola EI; Timonen S; Pakkanen TT; Harkki O; Seppala JV Functional surface groups for single-site heterogeneous alpha-olefin polymerization catalysts. *Appl. Surf. Sci* 1997, 121, 372–377.
- (8). Liu YH; Lin HP; Mou CY Direct method for surface silyl functionalization of mesoporous silica. *Langmuir* 2004, 20, 3231–3239. [PubMed: 15875852]
- (9). Deng G; Markowitz MA; Kust PR; Gaber BP Control of surface expression of functional groups on silica particles. *Mater. Sci. Eng., C* 2000, 11, 165–172.
- (10). Impens NREN; van der Voort P; Vansant EF Silylation of micro-, meso- and non-porous oxides: A review. *Microporous Mesoporous Mater* 1999, 28, 217–232.
- (11). Sutra P; Fajula F; Brunel D; Lentz P; Daelen G; Nagy JB ²⁹Si and ¹³C MAS-NMR characterization of surface modification of micelletemplated silicas during the grafting of organic moieties and end-capping. *Colloids Surf., A* 1999, 158, 21–27.
- (12). Kim S; Gavalas GR Kinetic study of the reactions of chlorosilanes with porous vycor glass. *J. Colloid Interface Sci* 1993, 161, 6–18.
- (13). Rubinsztajn S; Cypryk M; Chojnowski J Condensation of model linear siloxane oligomers possessing silanol and silyl chloride end groups. The mechanism of silanol silylation by a chlorosilane in the presence of neutral nucleophiles. *J. Organomet. Chem* 1989, 367, 27–37.
- (14). Lazghab M; Saleh K; Guigon P A new solventless process to hydrophobize silica powders in fluidized beds. *AIChE J* 2008, 54, 897–908.
- (15). Bogart GR; Leyden DE Investigation of amine-catalyzed gas-phase adsorption silylation reactions with alkoxy silanes. *J. Colloid Interface Sci* 1994, 167, 27–34.
- (16). Feng X; Fryxell GE; Wang LQ; Kim AY; Liu J; Kemner KM Functionalized monolayers on ordered mesoporous supports. *Science* 1997, 276, 923–926.
- (17). Walcarius A; Delacote C Mercury(II) binding to thiol-functionalized mesoporous silicas: Critical effect of pH and sorbent properties on capacity and selectivity. *Anal. Chim. Acta* 2005, 547, 3–13.
- (18). Nooney RI; Kalyanaraman M; Kennedy G; Maginn EJ Heavy metal remediation using functionalized mesoporous silicas with controlled macrostructure. *Langmuir* 2001, 17, 528–533.
- (19). Mercier L; Pinnavaia TJ Heavy metal ion adsorbents formed by the grafting of a thiol functionality to mesoporous silica molecular sieves: Factors affecting Hg(II) uptake. *Environ. Sci. Technol* 1998, 32 (18), 2749–2754.

- Author Manuscript
- Author Manuscript
- Author Manuscript
- Author Manuscript
- (20). Mahmoud ME; El-Essawi MM; Kholeif SA; Fathalla EMI Aspects of surface modification, structure characterization, thermal stability, and metal selectivity properties of silica gel phases-immobilized amine derivatives. *Anal. Chim. Acta* 2004, 525, 123–132.
 - (21). Han DM; Fang GZ; Yan XP Preparation and evaluation of a molecularly imprinted sol-gel material for on-line solid-phase extraction coupled with high performance liquid chromatography for the determination of trace pentachlorophenol in water samples. *J. Chromatogr. A* 2005, 1100, 131–136. [PubMed: 16188266]
 - (22). Yang LM; Wang YJ; Luo GS; Dai YY Functionalization of SBA-15 mesoporous silica with thiol or sulfonic acid groups under the crystallization conditions. *Microporous Mesoporous Mater* 2005, 84, 275–282.
 - (23). Makkuni A; Varma RS; Sikdar SK; Bhattacharyya D Vapor phase mercury sorption by organic sulfide modified bimetallic iron-copper nanoparticle aggregates. *Ind. Eng. Chem. Res* 2007, 46, 1305–1315.
 - (24). Makkuni A; Bachas LG; Varma RS; Sikdar S; Bhattacharyya D Aqueous and vapor phase mercury sorption by inorganic oxide materials functionalized with thiols and poly-thiols. *Clean Technol. Environ. Policy* 2005, 7, 87–96.
 - (25). Switaj-Zawadka A; Konieczka P; Szczygelska-Tao J; Biernat JF; Namiesnik J New procedure of silica gel surface modifications Preparation of gaseous standard mixtures for calibration purposes. *J. Chromatogr. A* 2004, 1033, 145–151. [PubMed: 15072299]
 - (26). Lee JY; Ju YH; Keener TC; Varma RS Development of cost-effective noncarbon sorbents for Hg(0) removal from coal-fired power plants. *Environ. Sci. Technol* 2006, 40, 2714–2720. [PubMed: 16683613]
 - (27). Pitoniak E; Wu CY; Mazyck DW; Powers KW; Sigmund W Adsorption enhancement mechanisms of silica-titania nanocomposites for elemental mercury vapor removal. *Environ. Sci. Technol* 2005, 39, 1269–1274. [PubMed: 15787366]
 - (28). Srivastava RK; Hutson ND; Martin B; Princiotta F; Staudt J Control of mercury emissions from coal-fired electric utility boilers. *Environ. Sci. Technol* 2006.
 - (29). Hutson ND; Attwood BC; Scheckel KG XAS and XPS characterization of mercury binding on brominated activated carbon. *Environ. Sci. Technol* 2007, 41, 1747–1752. [PubMed: 17405227]
 - (30). Abu-Daibes MA; Pinto NG Synthesis and characterization of a nano-structured sorbent for the direct removal of mercury vapor from flue gases by chelation. *Chem. Eng. Sci* 2005, 60, 1901–1910.
 - (31). Meyer DE; Sikdar SK; Hutson ND; Bhattacharyya D Examination of sulfur-functionalized, copper-doped iron nanoparticles for vapor-phase mercury capture in entrained-flow and fixed-bed systems. *Energy Fuels* 2007, 21, 2688–2697.
 - (32). Meyer DE; Meeks N; Sikdar S; Hutson ND; Hua D; Bhattacharyya D Copper-doped silica materials silanized with bis-(triethoxy silyl propyl)-tetra sulfide for mercury vapor capture. *Energy Fuels* 2008, 22, 2290–2298.
 - (33). Sing KSW; Everett DH; Haul RAW; Moscou L; Pierotti RA; Rouquerol J; Siemieniewska T Reporting Physisorption Data for Gas Solid Systems with Special Reference to the Determination of Surface-Area and Porosity (Recommendations 1984). *Pure Appl. Chem* 1985, 57, 603–619.
 - (34). Boccuzzi F; Coluccia S; Ghiotti G; Morterra C; Zecchina A Infrared study of surface modes on silica. *J. Phys. Chem* 1978, 82, 1298–1303.
 - (35). Cestari AR; Airoldi C A new elemental analysis method based on thermogravimetric data and applied to alkoxy silane immobilized on silicas. *J. Therm. Anal* 1995, 44, 79–87.
 - (36). Hohne GWH; Hemminger WF; Flammersheim H-J *Differential Scanning Calorimetry*; 2nd ed.; Springer-Verlag: New York, 2003; Vol. 1, p 298.

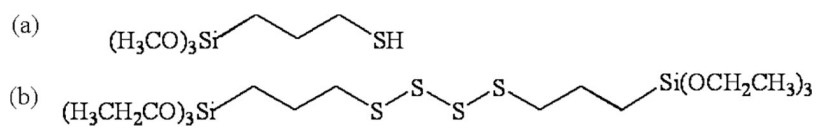


Figure 1. Silanes used in the synthesis of sulfur-functionalized silica particles: (a) 3-mercaptopropyl trimethoxy silane (MPTMS); (b) bis[3-(triethoxysilyl) propyl]-tetrasulfide (S4).

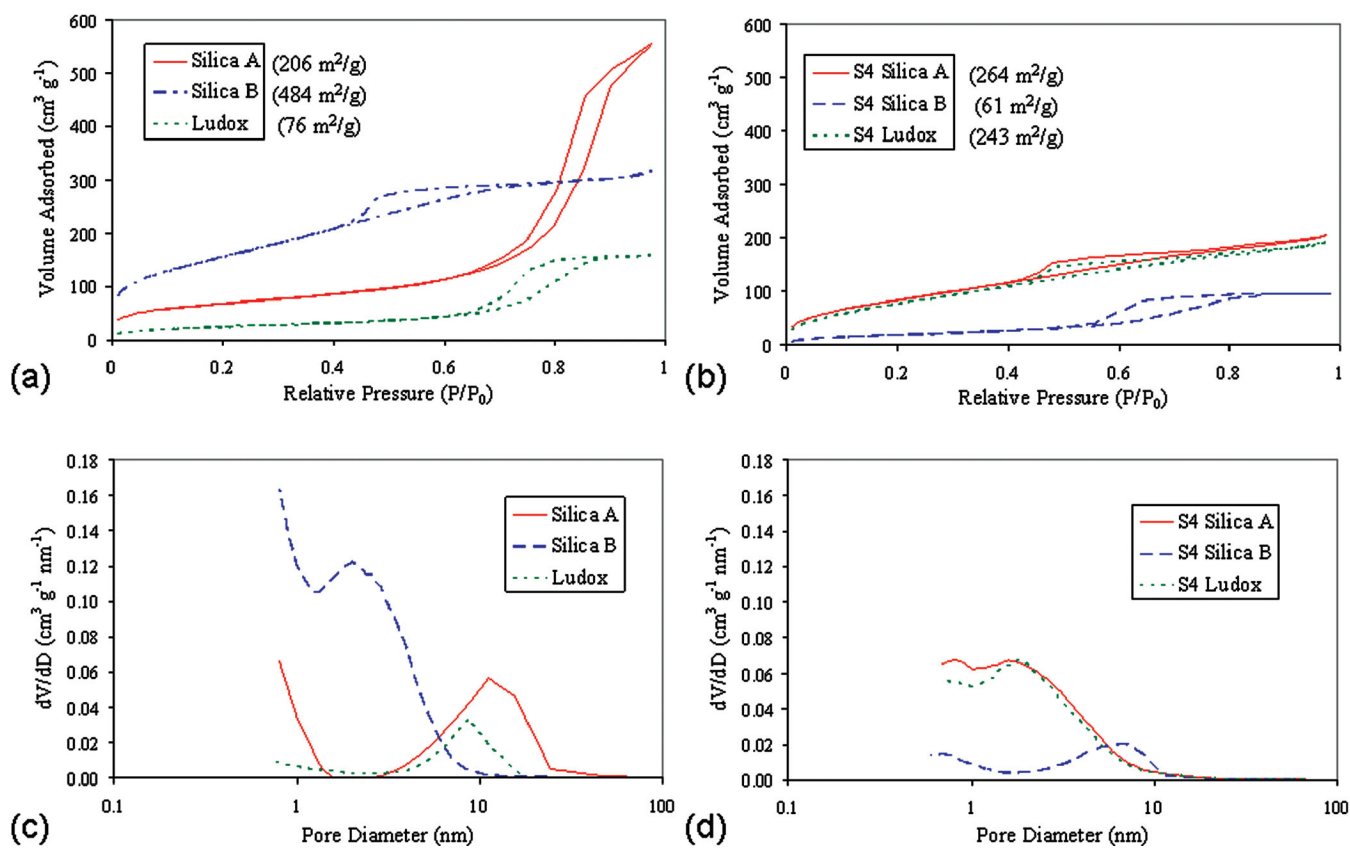


Figure 2. Nitrogen adsorption isotherms at 77 K for (a) unfunctionalized and (b) functionalized silica particles. Pore volume distributions for (c) unfunctionalized and (d) functionalized silica particles.

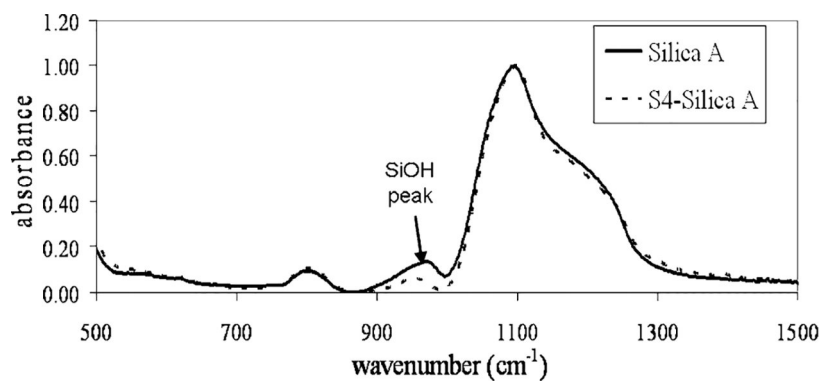


Figure 3. Representative FTIR spectra of S4-functionalized silica. The transmission FTIR peak at 980 cm^{-1} is attributed to the Si–O–H vibration, and its relative height can be used to determine the extent of silylation reaction. The decrease in peak height after functionalization is seen here for S4-silica A (54% of silanol groups functionalized).

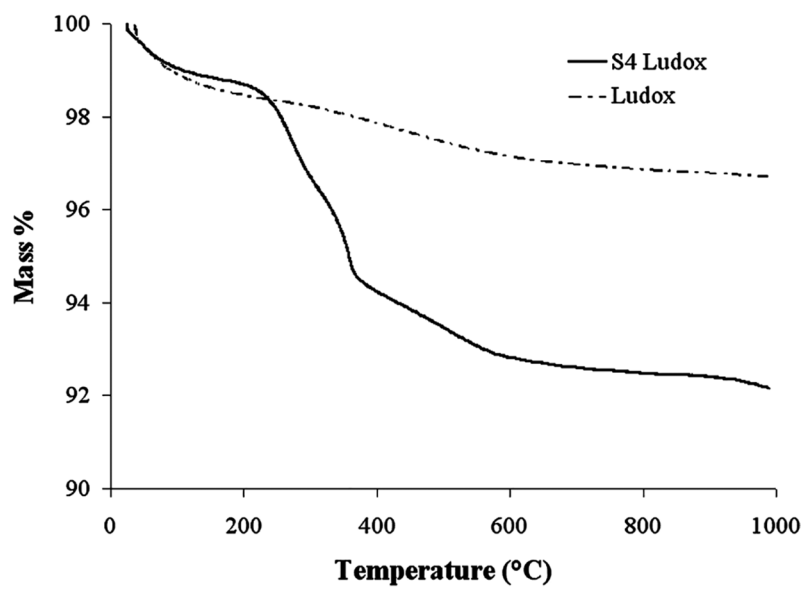


Figure 4. Representative TGA plot which shows mass loss difference for silica and S4 functionalized silica. This plot shown for Ludox and S4-Ludox sample.

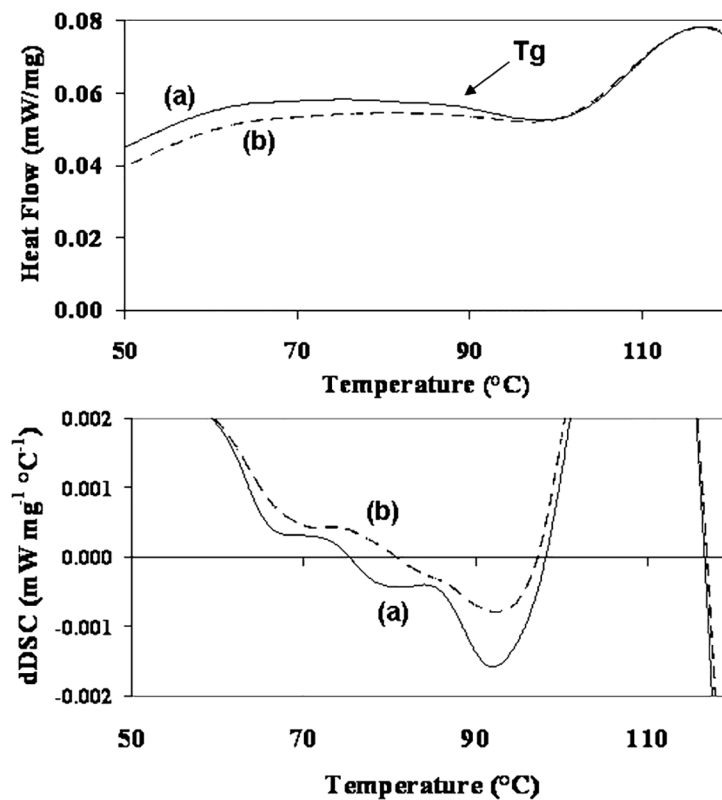


Figure 5. Differential scanning calorimetry demonstrates thermal transitions of (a) S4-silica A particles and (b) MPTMS-functionalized particles. These *cooling* scans were obtained by heating to 130 °C in order to remove excess moisture then cooled to 30 °C. Parameters: cooling rate of 5 °C min⁻¹; Pt-Rh alloy pan; N₂ atm. The baseline DSC plot for an empty pan was subtracted. A slight glass transition (T_g) is observed at about 85 °C for the S4 functionalized particles, as also confirmed by the DSC derivative plot.

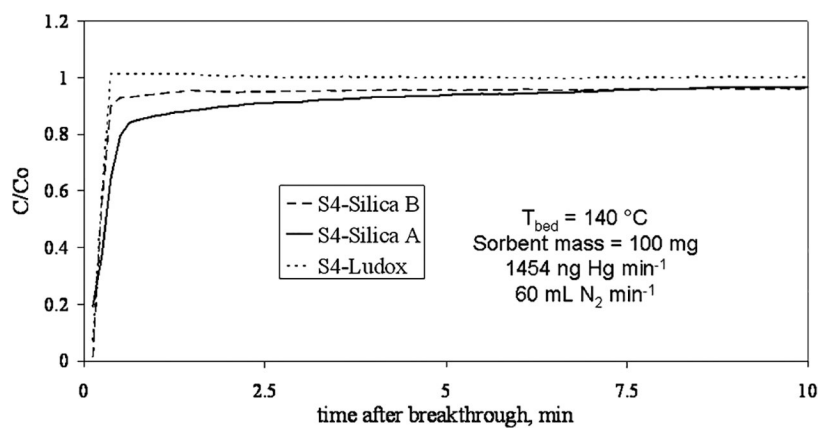


Figure 6. Breakthrough curves for packed bed of mercury sorbents. Steeper and sharper breakthrough curves indicate the material is more open structured, with less mass transfer resistance.

Table 1.

Pore Diameters and Surface Areas of Silica Particles before and after S4-Functionalization. Silicas A and B Are Amorphous Silica Gel Particles and Ludox Is a Colloidal Silica Particle Which Has a Nonporous Base Particle

silica sample	unfunctionalized silica			S4-functionalized silica		
	average particle diameter (μm)	average pore diameter (nm)	surface area ($\text{m}^2 \text{g}^{-1}$)	average pore diameter (nm)	surface area ($\text{m}^2 \text{g}^{-1}$)	surface area ($\text{m}^2 \text{g}^{-1}$)
silica A	3.7	9.6	206	3.3	264	264
silica B	3.3	2.9	484	4.7	61	61
Ludox	0.022	7.1	76	3.2	243	243

Table 2.

Summary of Silylation Results with Experimental Method

silica type	silane	% silanol functionalized (IR)	mass % silane (TGA)	mass % sulfur (TSA)
silica B	MPTMS	38	10.6	3.99
silica A	S4	54	12.0	4.53
silica B	S4	17	11.0	3.98
Ludox	S4	NA	4.7	1.56

Author Manuscript

Author Manuscript

Author Manuscript

Author Manuscript